Natural Resources for Human Health

Phenolic compounds as antiviral agents: An In-Silico investigation against essential proteins of SARS-CoV-2

Hammami Majdi [1,*], Feten Zar Kalai [1], Walid Yeddes [1], Moufida Saidani [1]

[1]Laboratory of Medicinal and Aromatics Plant, Biotechnology Center of Borj-Cedria, BP 901, 2050 Hammam-Lif, Tunisia

ABSTRACT: Plant biodiversity is endowed with a huge composition and variability of active molecules known for their therapeutic effects against several diseases. In this current work, several phenolic compounds are subject of in silico evaluation of their interactions with six severe acute respiratory syndrome coronavirus (SARS-CoV) enzymes to evaluate the binding mode and mechanism of phenolic compounds interactions with SARS-CoV-2 enzymes. Results of molecular docking and data analysis revealed that the importance of interactions was dependent to the phenolic class of tested ligand; tannin, biflavone and flavonoid glycoside were the most interactive classes. Among the top three ranked molecules recording lower binding energy against each virus protein target, In conclusion, it was found that Amentoflavone, Dieckol, Bilobetin, Punicalagin, Tellimagrandin-I, Tannic acid, Sciadopitysin, Ginkgetin and Chebulagic acid could be a promising antiviral drug since they present more important binding energy than conventional ones. Their interactions were justified by the Wenn diagram and Ramachandran plot. However, these phenolic compounds recorded an important bioavailability score and found fulfilling most of the drug-likeness criteria such as Lipinski's rule. Clearly, all observations point to further required works aiming to examine more deeply the possibility of using these molecules that could be probably a subject of pre-clinical studies.

1. INTRODUCTION

The pandemic of Covid-19 is of an arising contagious affection, called coronavirus affection 2019 or Covid-19, caused by the coronavirus SARS-CoV-2 (Hui et al., 2020), which appeared in Wuhan City on November 17th, 2019, in central Chinese (Hubei Province), before spreading in numerous countries. The World Health Organization (WHO) first warnings the People's Republic of China and its other member countries, and also declares a state of public health exigency of transnational concern on January 30th, 2020. On March 11th, 2020 (Chauhan, 2020), the new infection caused by this virus was confirmed as a pandemic by the WHO, which called for crucial protecting measures to prevent the overload of intensive care services and to reinforce precautionary hygiene avoidness of all physical contact kinds between people. Promotion of social distancing, and prohibition of crowds and major events as well as several travel restrictions, making people more aware about hand washing as a crucial step of preventive measures, implementation of quarantine, etc. In the whole world, countless cancellations of sport and cultural events was causing by this world-wide pandemic, several countries have put in place containment measures to slow down the appearance of new sources of contagion, even through the closure of their borders. Moreover, the spread of this pandemic had a negative impact on the social life of people as well as on the global economic stability since it has further slowed down the social and economic activities (Chauhan, 2020).

Currently, there are a little approved treatment that can treat the infection caused by SARS-CoV-2, consequently, there is an urgent claim for more chemotherapeutic agents to stop this disease.

Coronaviruses (CoVs) are single-stranded positive-sense RNA viruses that have enormous viral RNA genomes (V'kovski et al., 2020). Several works have shown that SARS-CoV-2 has a comparable genomic structure to that of beta-coronaviruses (Andersen et al., 2020; Chauhan, 2020). It consist of a 5′-untranslated region, a replicase complex that encode non-structural proteins, a spike protein gene, envelope protein gene, a membrane protein gene, a nucleocapsid protein gene, and numerous unidentified non-structural open reading frames (Islam et al., 2020; Qamar et al., 2020). Therefore, and like other beta-coronaviruses, this virus can be terminated by blocking these proteins. Chloroquine, hydroxychloroquine, lopinavir/ritonavir, favipiravir, remdesivir, nitazoxanide, and

---

* Corresponding author.
 E-mail address: hammamimajdi@hotmail.com (Hammami Majdi)

ivermectin were the commonly used drugs, they have showed their efficacy in inhibiting SARS-CoV-2 (Yavuz & Ünal, 2020). Those agents can selectively and potently inhibit some nonstructural proteins like; the Main protease and Helicase (Nsp13) (M^{pro}) Jin et al. (2020), Papain-like protease (PL^{pro}) (Rut et al., 2020) and structure proteins like (Xia et al., 2020); protein S, protein E and protein M. Hence, the search for new molecules with certain inhibitory activity is very extensive and gaining interest of researchers to test new molecules. In many previous studies, bioactive molecules originated from natural resources have been proven to possess a potential antiviral activity. In the present study, the main idea is to focus on making a computational simulation of inhibition effects of some phenolic compounds using Protein-Ligand Molecular Docking approach. In recent years, the development of drugs through mathematical and computational approaches has become increasingly (Alamri et al., 2020; Bobrowski et al., 2020; Nukoolkarn et al., 2008) .

2. MATERIALS AND METHODS

2.1. Proteins sequence preparation

For this work, four enzymes are chosen as targets:

Main protease (M^{pro}) downloaded from the PDB database encoded by 6LU7 (Jin et al., 2020) in a resolution of 2.16Å, is also called chymotrypsin-like protease ($3CL^{pro}$). It is responsible for cleaving most of the polyprotein sites and the results are non-structural proteins (nsps) that come together in the replicase-transcriptase complex (RTC).

Papain-like protease (PL^{pro}) taken from the PDB database with code of 6WUU (Rut et al., 2020) with a resolution of 2.79Å, cleaves the nonstructural protein 1-2, 2-3 and 3-4 boundaries and works with main protease to cleave the polyproteins into nsps.

Helicase (Nsp13) catalyses the unwinding of duplex oligonu-cleotides into single strands in an NTP-dependent manner. The SARS-CoV-2 helicase X-ray structure was built based on 6JYT (Jia et al., 2019) ccode in a resolution of 2.80Å. Therefore, the ADP binding site (ADP site), and the nucleic acids binding site (NCB site) were defined for small molecule docking.

RNA-dependent RNA polymerase (RdRP) downloaded from the PDB database with code of 7BV2 in a resolution of 2.50Å, catalyses the RNA replication from an RNA template (Venkataraman et al., 2018). Specially, it catalysis the RNA strand complementary synthesis to give template of RNA. This contrasts with typical DNA-dependent RNA polymerases, which used by all organisms to catalyse the transcription of RNA from a DNA template. Thus, we defined two docking sites: the RTP site, and the RNA site.

2.2. Ligand database preparation

156 phenolic compounds and 9 antiviral drugs were downloaded in three-dimensional (3D) illustration and SDF structural data format from open database of National Institutes of Health (https://pubchem.ncbi.nlm.nih.gov/) (Kim et al.,

2016). All these molecules are chosen by their reported antiviral activities against several viruses as following; African swine fever virus (ASFV) , Respiratory syncytial virus (RSV), Echovirus, Enterovirus A71 (EV-A71), influenza A virus subtype H1N1 (A/H1N1), Influenza A virus subtype H6N1 (A/H6N1), hepatitis C virus (HCV) , human immunodeficiency virus (HIV), human respiratory syncytial virus (hRSV), Herpes Simplex (HSV-1 & HSV-2), Porcine epidemic diarrhoea virus (PEDV), severe acute respiratory syndrome coronavirus (SARS-CoV) (**Table S1**, Appendix A Supplementary material).

2.3. Docking protocol

The proteins structures were downloaded as a Protein database files and then transformed into Protein Data Bank Partial Charge (PDBQT) format via MGLTools software (Trott & Olson, 2010). Before docking, polar-hydrogen atoms were included, and gasteiger charges were processed (Kong et al., 2020). Autodock-vina was used carried out to the structure-based virtual screening; the docking box was defined as the center of native ligand coordinates with 30Å×30Å×30Å in length to include the residues of complete cavity. MGLTools was used to add hydrogens and prepare pdbqt files for proteins and ligands with an exhaustiveness level at 12. The 2D interaction was generated using the LIGPLOT$^+$ software. The validation of the best generated model was done by analysis of Ramachandran plot generated in Ramachandran Plot server (https://zlab.umassmed.edu/bu/rama/).

2.4. Drug-likeness analysis by ADMET profiling

Absorption, distribution, metabolism, excretion, and tox-icology (ADMET) were performed online by SwissADME tools (Daina et al., 2017) (http://www.swissadme.ch/index.php). Drug-likeness can provide the possibility for a phenolic compounds to be developed as an oral drug with respect to bioavailability by the assessment of The Lipinski (Lipinski et al., 1997), Ghose (Ghose et al., 1999), Veber (Veber et al., 2002), Egan (Egan et al., 2000) and Muegge (Muegge et al., 2001) rule's.

2.5. Statistical analysis

Frequency distribution and heatmap were performed by orange software version 3.27.1 (Demšar et al., 2013), input data was generated from the (**Table S1**, Appendix A Supplementary material).

3. RESULTS AND DISCUSSION

3.1. Effect of phenolic class on docking scores

Figure 1 demonstrated that the distributions frequency of binding energy score among the different phenolic compounds and SARS-CoV-2 enzymes pre-selected varies between -5 and -12 kcal/mol. For Main protease, helicase (NCP site), RdRp (RNA site), the higher binding scores were recorded between -8 and -7 Kcal/mol with 56.41%, 48.72%, 52.56% respectively. As for the Helicase (ADP site), docking results show the lowest

Table 1

Binding scores (kcal/mol) of the top three phenolic compounds against each protein target

	Helicase (ADP site)		Helicase (NCP site)		RdRp (RNA site)
Amentoflavone	-9	Punicalagin	-10,9	Tannic acid	-10,6
Dieckol	-9	Tellimagrandin I	-10,9	Punicalagin	-10,8
Bilobetin	-8,9	Tannic acid	-10,8	Dieckol	-10,1
Ritonavir	-9,4	Ivermectin	-9,7	Ritonavir	-9,5
	Papain-like protease		**Main protease**		**RdRp (RTP site)**
Dieckol	-12,5	Sciadopitysin	-10,1	Dieckol	-12,6
Bilobetin	-11,3	Amentoflavone	-10	Chebulagic acid	-11,7
Amentoflavone	-11,2	Ginkgetin	-9,8	Tannic acid	-11,7
Indinavir	-10,2	Remdesivir	-8,4	Rupintrivir	-10,8

scores distributed with 46.79% between -6 and -7 Kcal/mol. 41.67% of binding scores were recorded at -8 and -9 Kcal/mol for papain like protease. Finally, the highest scores distribution characterize RdRp (RTP site) with 39.74% between -9 and -10 Kcal/mol. .

The result of a hierarchical k-means clustering (20 clusters) calculation is displayed in a heatmap (**Figure 2**) as a dendrogram, the row dendrogram shows the distance of similarity between rows, and which node belong to which row. As a result of clustering, **Figure 2-A** arranges the binding scores of ligands according to their phenolic classes (-5.011 and -12.60 kcal/mol), two principal clusters were manifested, the first (c1) regroups the high scores, the second regroups the low scores; ranging from -12 to -9 kcal/mol. Subcluster C1 generates four phenolic classes: tannins (Tannic acid, Tellimagrandin, Dieckol, Chebulagic acid, Pentagalloylglucose), biflavones (Amentoflavone, Bilobetin, Ginkgetin, Sciadopitysin), favan-3-ols (3-O-galloyl-procyanidin B2, Theaflavin) and flavonoid glycosides (Rhoifolin, Naringin, Neohesperidin, Hesperidin, Quercetin-3-O-rutinoside, Diosmin, Kaempferol-3-O-robinobioside, Kaempferol-3-O-rutinoside). Subcluster C2 contains: Abietane, Anthocyanidin, Anthraquinone, Benzopyrans, Chalcones, Coumarins, curcuminoids, Flavanones, Flavanonols, Furanoflavonoids, Geranylated flavonoids, Glycosylated Lignans, Glycosylated Phenylpropanoids, Iridoid Glucoside, Isoflavanes, Isoflavanone, Isoflavones, Isoprenylated flavan, acid Phenols, Phenylflavonoids, Phenylpropanoids, prenylflavonoid, stilbenoids, xanthonoid.

Phenolic acids show the highest binding scores close to -6 kcal/mol as an average. Consistently, previous docking simulations studies suggest the possibility that plant phenolic compounds can inhibit the responsible key factors r for the coronavirus life cycle (Russo et al., 2020). F. Chen et al. (2004) showed that the flavones glycosides have a potential anti-viral activity. In this work, ten SARS-CoV viruses were isolated from ten patients, Baicalin showed a half maximal effective concentration ranged from 12.50 to 25.00 μg/ml at 48 hours without significantly cell viability affection. In the same context, tetra-O-galloyl-β-d-glucose and luteolin, showed inhibitory activity for the entry process of SARS-CoV into host cells (Yi et al., 2004). These findings revealed that, biflavone and tannins class present an important binding energy score, which

are somehow consistent with other empirical studies (Khalifa et al., 2020; Ryu et al., 2010). The outcomes of our study led us to go further steps; mainly, the study of binding profile and the correlation between amino acid's proteins and proposed ligands.

3.2. Analysis of screened inhibitor interaction

To comprehend the binding mode of flavonoids interactions with SARS-CoV-2 enzymes, 156 phenolic compounds and 9 antiviral drugs were selected from literature. 9900 docking assays were conducted (including the replications to validate molecules binding energy scores). Following the ligands docking, many scores was established for all six-target proteins. The found results were set in rising score values order (**Table S1**, Appendix A Supplementary material). To simplify this work, the top three molecules against each target were selected (**Table 1**).

3.2.1 *Main protease (Mpro as a target*

Main protease (M^{pro}) is a potential pharmacological target against SARS CoV-2. It is a vital virus enzyme since it is indispensable for polyproteins proteolytic processing (Estrada, 2020). It is responsible for cleaving most of the polyprotein sites and the results are non-structural proteins (nsps) that come together in the replicase-transcriptase complex (RTC).

According to docking results (**Table S1**, Appendix A Supplementary material), the highest binding energy scores were recorded for biflavone, flavan-3-ols, flavonol glycoside, flavanone glycoside, flavonol glycoside, flavone glycoside, Tannins. 16.66% of tested ligands (26 phenolic compounds) have a score value superior to Remdesivir one used as a target control (Score Value: 8.4 kcal/mol), the top three ranked compounds against M^{pro} were compiled in **Table 1.**

Sciadopitysin has the best binding score (-10.1 kcal/mol), it is an active component that can be extacted from *Taxus chinensis* (Gu et al., 2013) , *Ginkgo biloba* (Liu et al., 2018), *Torreya nucifera* Ryu et al. (2010). Sciadopitysin possess a large pharmacological activity such as phosphatase inhibitor of regenerating liver-3 (PRL-3) (S.K. Choi et al., 2006), inhibitor of the amyloid-beta (Aβ) peptide aggregation Gu et al. (2013) . Scientific report of Ryu et al. (2010) , demonstrated that biflavonoids from *Torreya nucifera* exhibited an important SARS-CoV 3CL^{pro} inhibitory activity (62%

Table 2
Drug-likeness analysis of the top three molecules against each target of SARS-Cov-2

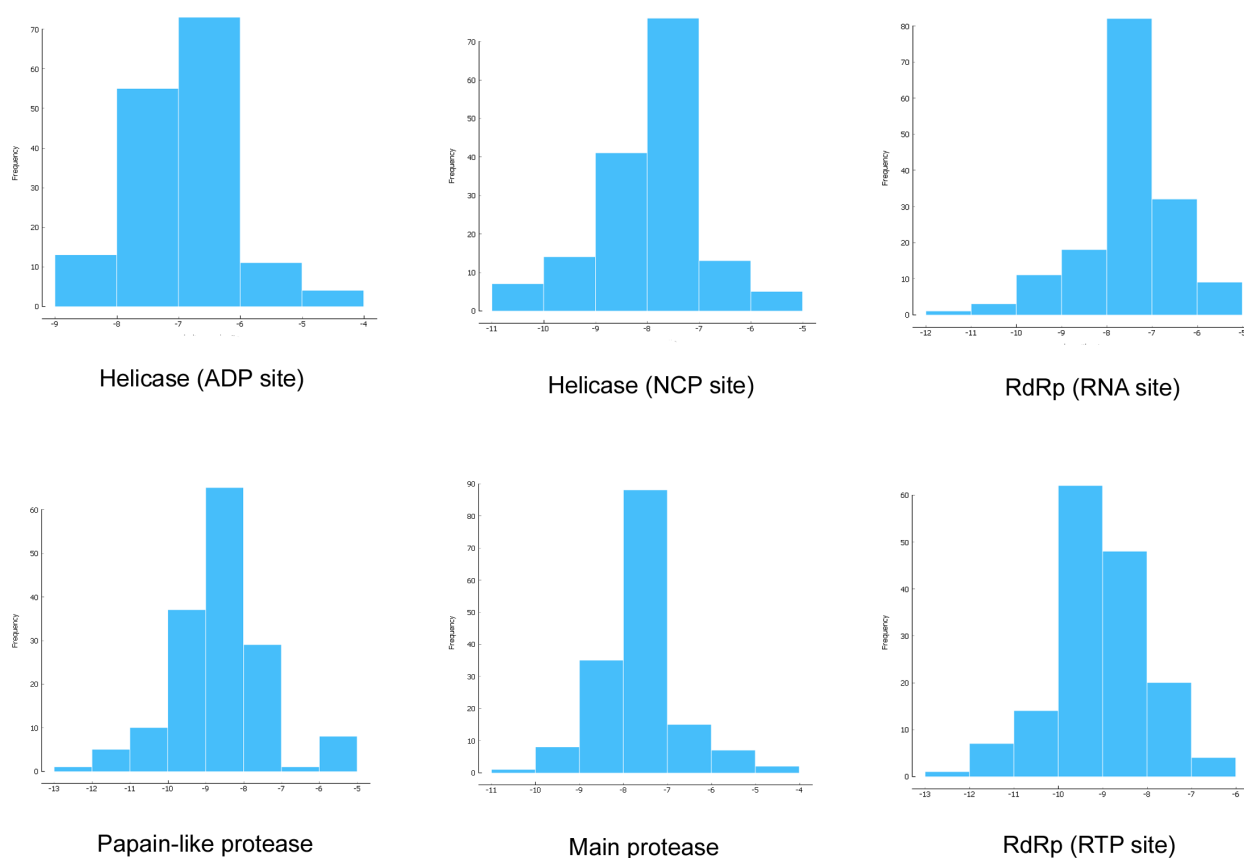| Ligands	Amentoflavone	Dieckol	Bilobetin	Punicalagin	Tellimagrandin I	Tannic acid	Sciadopitysin	Ginkgetin	Chebulagic acid
Physicochemical Properties									
MW (Da)	538.46	742.55	552.48	1084.72	786.56	1701.20	580.54	566.51	954.66
H-bond acceptors	10	18	10	30	22	46	10	10	27
H-bond donors	6	11	5	17	13	25	3	4	13
TPSA (Å²)	181.80	287.14	170.80	518.76	377.42	777.98	148.80	159.80	447.09
Lipophilicity									
iLOGP	3,06	2,66	3,39	0,77	0,91	2,9	4,65	3,94	0,24
Water Solubility									
Log S	-6.75	-7.61	-6.96	-8.05	-5.41	-12.61	-7.39	-7.17	-5.92
Solubility (mg/ml)	9.63e-05	1.83e-05	6.12e-05	9.73e-06	3.04e-03	4.16e-10	2.38e-05	3.82e-05	1.16e-03
Solubility (mol/l)	1.79e-07	2.46e-08	1.11e-07	8.97e-09	3.87e-06	2.45e-13	4.11e-08	6.75e-08	1.21e-06
Class	Poorly soluble	Poorly soluble	Poorly soluble	Poorly soluble	Moderately soluble	Insoluble	Poorly soluble	Poorly soluble	Moderately soluble
Druglikeness									
Lipinski #violations	2	3	1	3	3	3	1	1	3
Veber #violations	1	1	1	1	1	2	1	1	1
Bioavailability Score	0.17	0.17	0.55	0.17	0.17	0.17	0.55	0.55	0.11
Medicinal Chemistry									
PAINS #alerts	0	0	0	1	1	1	0	0	1
Brenk #alerts	0	0	0	4	2	3	0	0	3

Figure 1. Frequency distribution of scores classes by enzymes

at 100 μg/mL). Further, in our findings it was found that Sciadopitysin can realize 3 hydrogen bonds (HB) with Gly143(A): 3.18Å as a distance between residue and target, Thr26(A): 2.82Å, Thr26(A): 2.86Å and 13 hydrophobic interactions (HI); Glu166(A), Gln189(A), Arg188(A), Asp187(A), Met165(A), HIs164(A), His163(A), His41(A), Cys145(A), Leu27(A), Thr25(A), Asn142(A), Leu141(A). Similar studies on 3CL^{pro} interaction with sciadopitysin revealed a high binding score: 9.1kcal/mol (Augustin et al., 2020) and -9.2 kcal/mol (Rana et al., 2020).

Amentoflavone, the second ranked ligand of M^{pro} with -10 kcal/mol binding score is a biflavone (bis-apigenin coupled at 8 and 3' positions, or 3′,8″-biapigenin) originated from several plants including *Ginkgo biloba* (Lobstein-Guth et al., 1988), *Hypericum perforatum* (Michler et al., 2011), *Xerophyta plicata* (Williams et al., 1987). and *Chamaecyparis obtusa* (Krauze-Baranowska et al., 2005). Recently, it is proved to possess interesting activities, including protective antioxidant effects (Y.L. Li et al., 2020) and cyclooxygenases inhibitor (Banerjee et al., 2002). In virology, it has been reported that amentoflavone could reduce coxsackievirus B3 replication (Wilsky et al., 2012). Also, it showed strong antiviral activity against HSV-1 and ACV-resistant

strains F. Li et al. (2019). Results obtained by ligplot software disclosed that this biflavone interacts with M^{pro} protein through 3 hydrogen bonds: His163(A): 3.16Å, Thr26(A): 3Å, Thr26(A): 3.08Å, and 14 hydrophobic interactions: His41(A), Gln189(A), Arg188(A), Gln166(A), Met165(A), Asp187(A), His164(A), Leu141(A), Ser144((A), Thr25(A), Gly143(A), Leu27(A), Cys145(A), Ans142(A). Rameshkumar et al. (2021) reported that amentoflavone exhibited a binding affinity with a score of −8.1 kcal/mol against main protease. Consistently, additional work done on biflavonoids of *Torreya nucifera* leaves showed that amentoflavone had −9.2 kcal/mol binding affinity (Ghosh et al., 2020).

Ginkgetin a biflavonoid derived from leaves of *Ginkgo biloba* (Son et al., 2005), *Selaginella moellendorffii* (Sun et al., 1997), *Taxus chinensis* (Ruan et al., 2014), ginkgetin exhibit numbers of pharmaceutical activities (Adnan et al., 2020) including antiinflammatory, antibacterial, leishmanicidal and antiplasmodial agent, antifungal, and antitumor activities (Lou et al., 2017). This bioflavonoid is the third best ligand with -9.8 kcal/mol, can realize 3 HB; Asn142(A): 2.78Å, Thr26(A): 3.11Å, Thr26(A):3.05Å and 16 Hydrophobic interactions; Met165(A), Cys145(A), Gln189(A), His164(A), Arg188(A), sp187(A)   , Thr25(A), His41(A), leu27(A), Ser144(A),
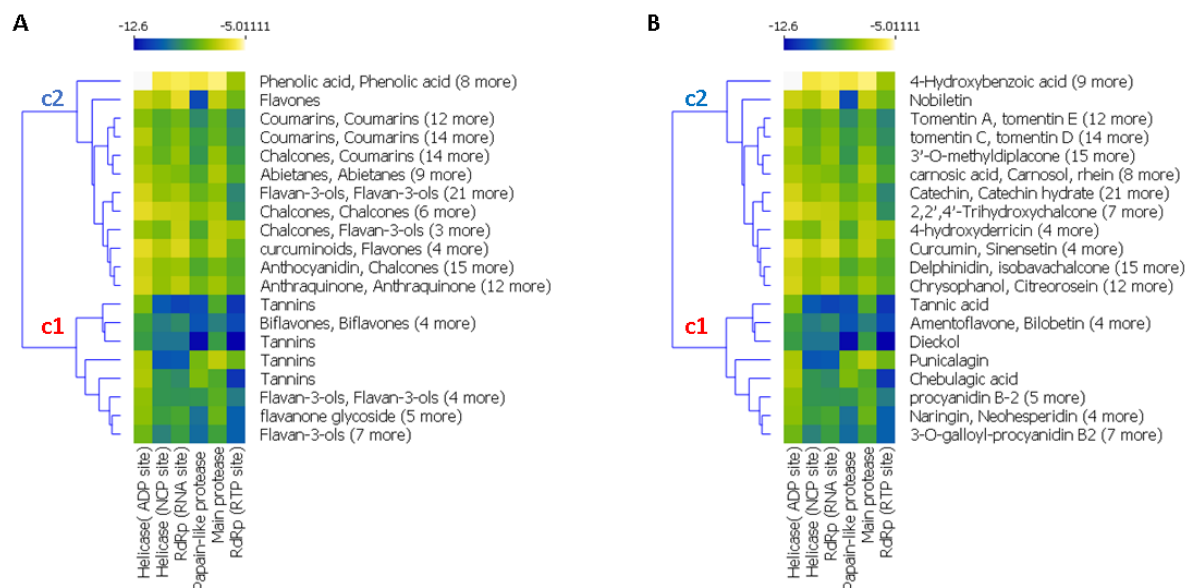
Figure 2. Heatmap clustering of phenolic compound: A by chemical classes, B by compounds.

Leu141(A), Gly143(A), His163(A), His172(A), Glu166(A), Phe140(A). These present findings are concordant with the work of Rana et al. (2020) reporting that ginkgetin interact with main protease and have a potential docking binding score (-10.19 kcal/mol). There are 8 residues are in common shown in the Wenn diagram (**Figure 5**); Hr26(A), His41(A), Gln189(A), Arg188(A), Met165(A), Leu141(A), Gly143(A), Cys145(A). All the residues were confirmed with amino acid listed in Main protease active site (**Table S2**, Appendix A supplementary data). Data presented in this table, show that the phenolic compounds can occupy the predicted active site of the protein M^{pro}, and the stability of the protein-ligand complexes is ensured by the comparison of the stereochemical structures of these molecules by carrying out by Ramachandran Plot (**Figure 4**). The latter is used to validate the protein structure based on the φ (phi), ψ (psi) and ω (omega) angles values. The plots revealed that the structure of the protein remains intact even in complex with the three molecules. The RMSD of backbone alpha carbon atoms of Amentoflavone-Main^{Pro}, and ginkgetin main protease complex were reported recently by Ghosh et al. (2020) . The average RMSD values (computed from five independent analysis) for unligated M^{pro}, M^{pro}-amentoflavone, and M^{pro}-ginkgetin complexes were found to be 0.297nm, 0.248nm and 0.246nm, respectively, suggesting that these two ligand-complexes were stable.

3.2.2 Papain-like protease (PLpro as a target

The papain-like protease (PL^{pro}) is an interesting antiviral target because they are essential for the replication of coronaviruses (Shin et al., 2020), PL^{Pro} is a protease located in NS3 of the viral polypeptide, in addition, PL^{pro} remove ubiquitin and ISG15 from the proteins of the host cell to help viruses evade innate host immune responses. Following a docking analysis of nine commercialized drugs, results revealed that Indinavir exhibited a higher binding score (-10.3 kcal/mol) for that it has been selected as the best control ligand. Fifteen phenolic compounds have a superior score values and the top three ranked were Dieckol, Bilobetin, Amentoflavone with score value: -12.5, -11.3 and -11.2 kcal/mol respectively (**Table 1**).

Dieckol, a phlorotannin, extracted from brown seaweed; *Eisenia bicyclis* (Koirala et al., 2017), Ecklonia cava (Moon et al., 2011). It is known to act as antibacterial activity (J.S. Choi et al., 2014), UVB-photoprotective activity (Guinea et al., 2012), anti-inflammatory (Sanjeewa et al., 2020) and cytoprotective agents (Lee et al., 2013). The antiviral activities of dieckol have been largely reported. Such as, *in vitro* antiviral activity of this active compound against murine norovirus (MNV) in RAW 264.7 cells has recorded EC_{50} of 0.90 μM (Eom et al., 2015). Additionally, it possesses an important activity against Influenza A viruses; [H1N1], [H9N2] and [H3N2] (Ryu et al., 2011). Park et al. (2013) demonstrated that dieckol showed significant inhibitory against SARS-CoV $3CL^{pro}$ cell-free cleavage (IC_{50}= 2.7 μM). These previous
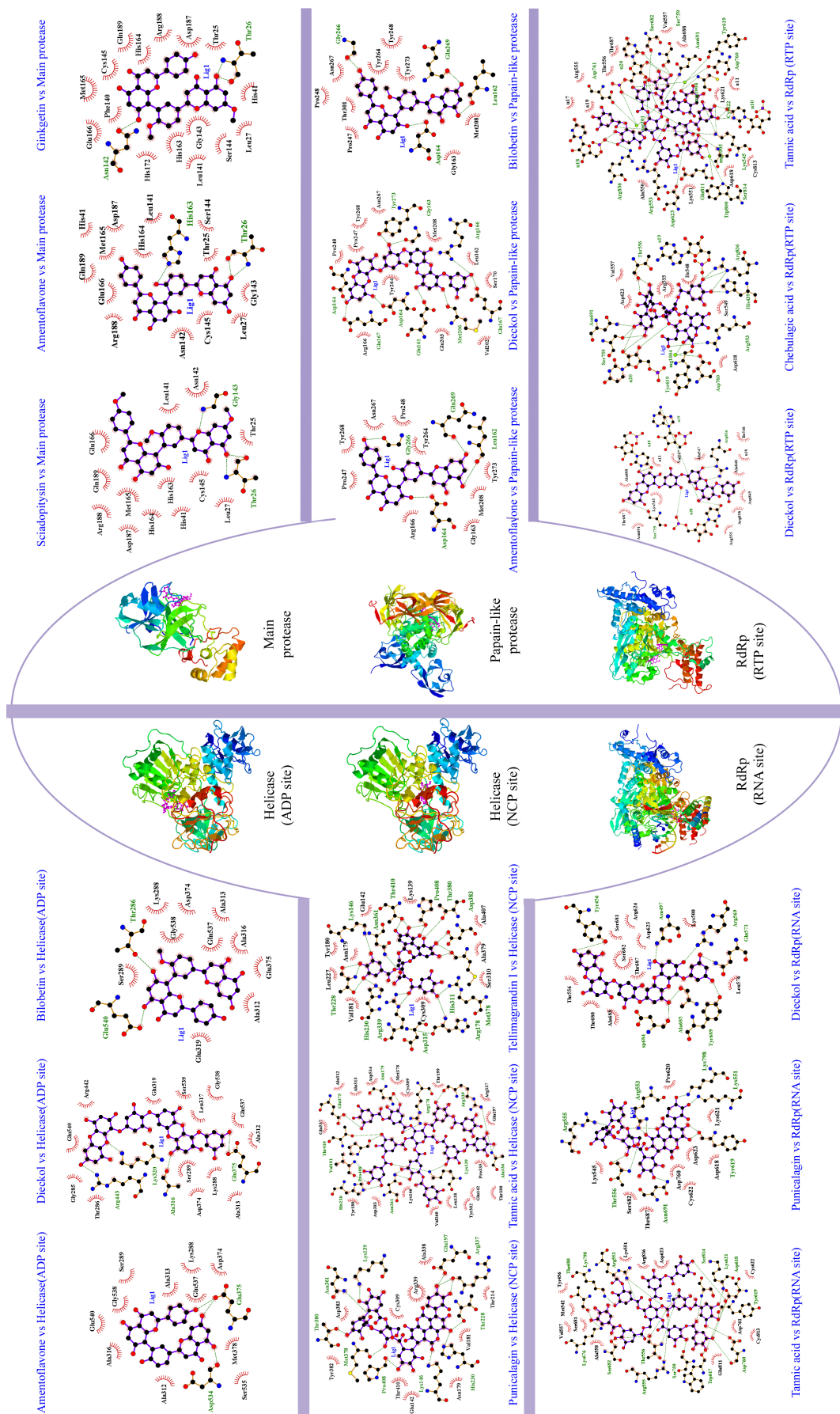
Figure 3. Binding modes and molecular interactions of screened compounds against SARS-CoV-2.
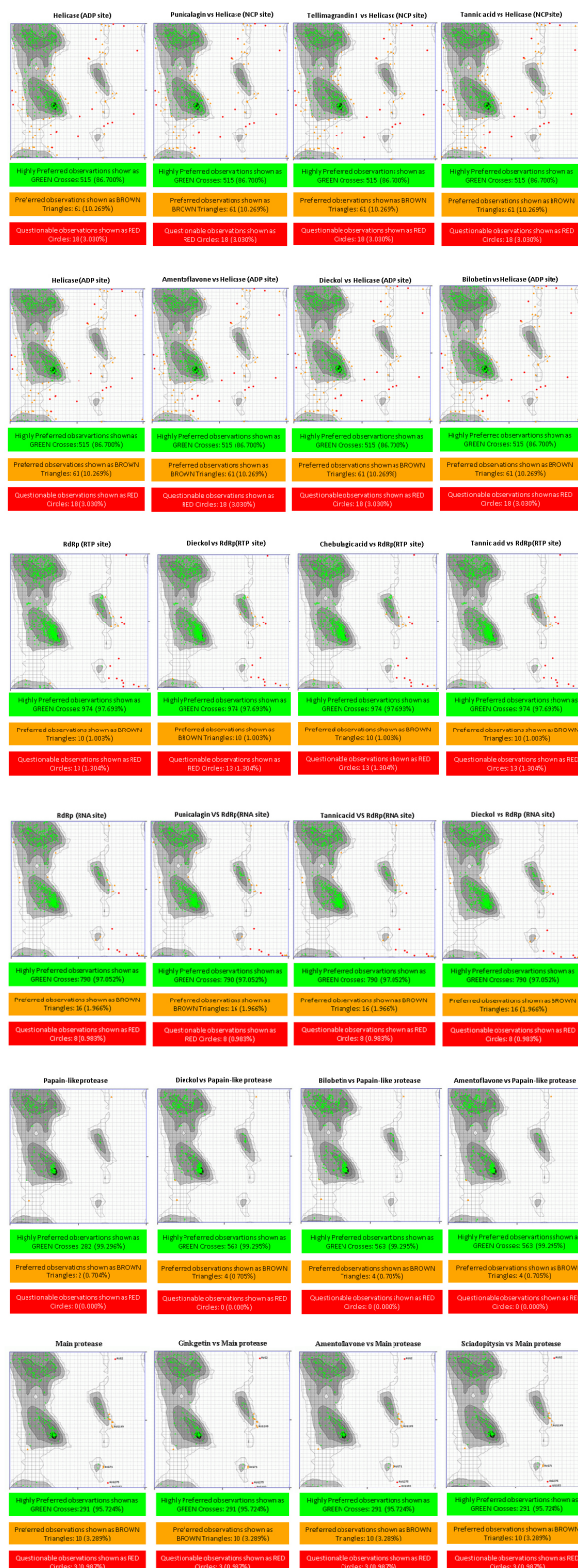
Figure 4. Comparison of stereochemical structures of ligand/protein complex by Ramachandran Plot.
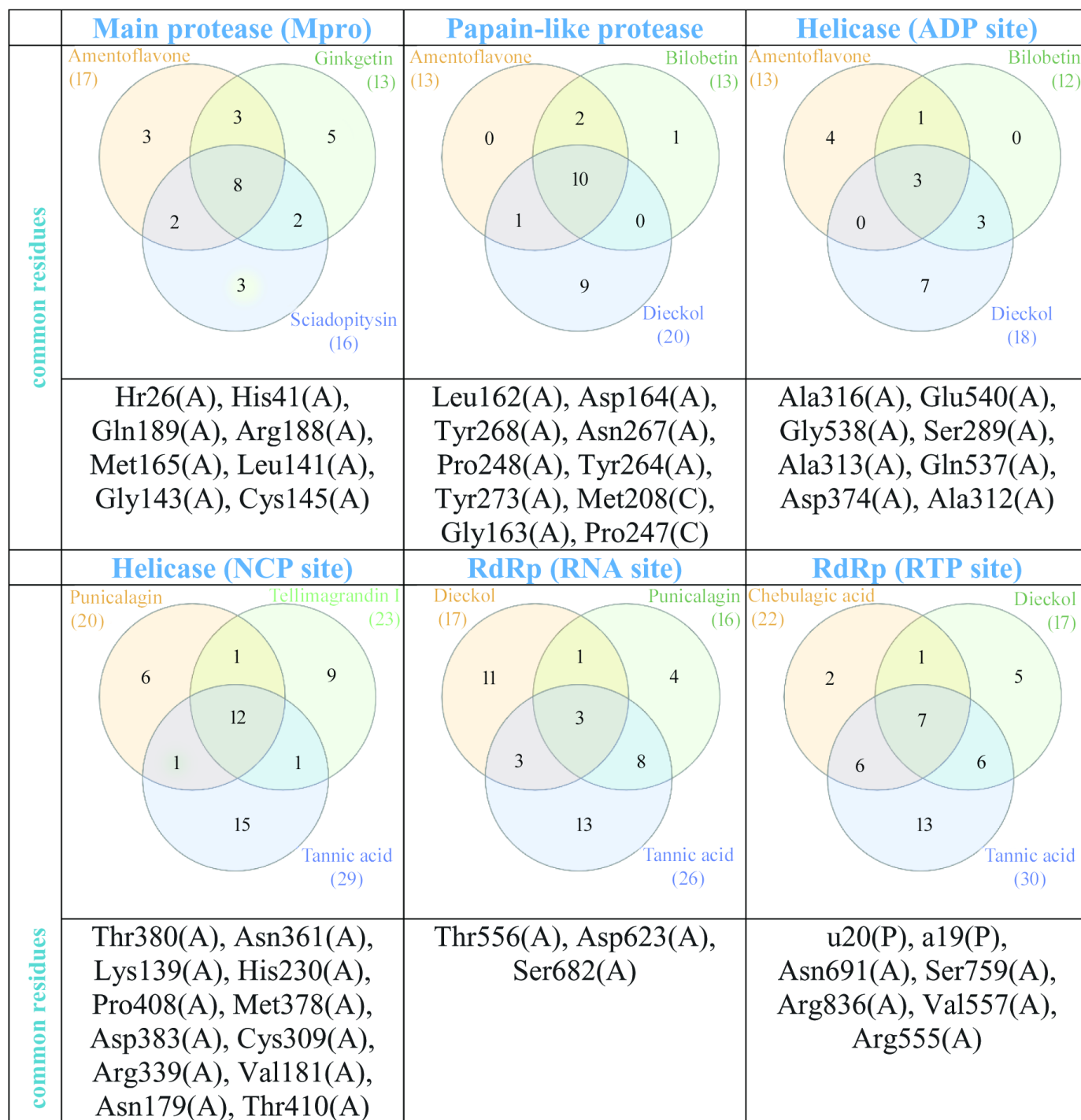
Figure 5. Wenn diagram of common residues by crossing the top three ranked phenolic compounds.

results encourage us to consider it as a potential drug candidate. Docking results revealed that this natural phlorotannin interacted through 8 HB; Asp164(C): 3.1Å, Glu167(C): 3.12Å, Asp164 (A): 2.69Å, Glu161(A): 2.83Å, Met206(C) 3.21Å, Glu167(A): 2.71Å, Arg166 (C): 3.22Å, Gly163(A):3.13Å, Tyr273(A): 2.7Å, Moreover, this compound also formed a large hydrophobic interactions network with the surrounding amino acids, including 11 residues; Pro248(A), Pro247(C), Tyr268(A), Asn267(A), Met208(C), Leu162(A), Ser170(C), Val202(C), Glu203(C), Tyr264(A), Arg166(A). Gentile et al. (2020) reported that dieckol was able to bind and inhibit the 3CL^{pro} due to an extensive network of HB (binding score: -12 kcal/mol).

Bilobetin is a biflavone extracted from *Ginkgo Biloba* L plants. Recently it was reported to present several biological activities such as an antiviral (Freitas et al., 2009), anticancer M. Li et al. (2219) , antinflammatory M. Li et al. (2019) , antibacterial (Woldemichael et al., 2003) and antifungal (Krauze-Baranowska & Wiwart, 2003). Moreover, several computational works showed that bilobetin is a vigorous drug candidate for the treatment of herpes simplex virus (HSV) and hepatitis B virus (HBV) infection (Ramaiah & Suresh, 2013). According to results summarized in **Table 1**, it was found that the estimated docking binding score for bilobetin was (-11.3kcal/mol). Based on this value, we have further extended our study to check the interactions network between 3CL^{pro} and bilobetin, Gly266(A): 2.89Å, Asp164(A): 3.04Å, Gln269 (A): 3.02Å, Leu162(A): 2.95Å represent the residues that interact with our ligand by hydrogen bonding, Asn267(A), Pro248(A), Thr301(A), Pro247(C), Tyr264(A), Tyr268(A), Tyr273(A), Met (208) C, Gly163 (A) were the amino acid having hydrophobic interactions with bilobetin. In similar study on PL^{pro} (PDB ID: 6W9C) (Rana et al., 2020), it has been consistently shown that bilobetin could interact with Pl^{pro} protein through 7 HB with the following residues: Phe 140, Glu166, Gln 189, Thr 190 and Gln 192. It could also form 3 hydrophobic interactions (Met 165, Glu 166 and Pro 168), recording a freen energy binding score of -10.83 Kcal/mol.

Amentoflavone, as described before, showed the third potent affinity to 3CL^{pro} (-11.2 kcal/mol), the 2D representation of ligand-protein binding including HB and HI are presented in **Figure 3**. Thirteen residues of 3CL^{pro} interacted with the ligand, 4 HB were formed between Amentoflavone and Gly266(A): 3.01Å, Gln269(A): 2.85Å, Leu162(A): 2.82Å, Asp164(A): 3.19Å, while, 9 amino acid residues, Tyr268(A), Asn267(A), Pro248(A), Tyr264(A), Tyr273(A), Met208(C), Gly163(A), Arg166(C), Pro247(C), formed hydrophobic interactions. This result was approved by a recent work, elucidating by SARS 3C-like protease inhibition assay and molecular docking study that amentoflavone was the most potent SARS-CoV 3CL^{pro} inhibitor with IC$_{50}$ = 8.3 μM (Abdillah & Cita, 2020). Moreover, the potential of the inhibitor amentoflavone correlated well with binding energies -11.42 kcal/mol, In the former, the interaction of this biflavone with the substrate-binding pocket of 3CL^{pro} involved 5 hydrogen bonds with:

His163 (3.154Å), Leu141 (2.966Å), Gln189 (3.033Å), Val186 (4.228Å) and Gln192 (3.898Å). Wenn diagram summarize the intersection between catalytic residues interactions, (**Figure 5**), Asp164 (A) formed hydrogen bonds with the three ligands studied in this work. Leu162(A), Tyr268(A), Asn267(A), Pro248(A), Tyr264(A), Tyr273(A), Met208(C), Gly163(A), Pro247(C) formed Hydrophobic interactions. All the residues were confirmed with amino acid listed in 3CL^{pro} active site (**Table S2**, Appendix A supplementary data). Highly Preferred observations shown in Ramachandran Plot (**Figure 4**) revealed that the interaction of ligands/enzymes do not affect the protein stereochemistry, which allows us to conclude that these complexes are stable and robust. In conclusion, of the results obtained, papain like protease can be considered as a potential target for SARS-CoV 2 inhibitors.

3.2.3 Helicase (Nsp13 as a target

The helicase is known as an enzyme that catalyze the NTP-dependent unwinding of duplex oligonucleotides into single strands (Kadaré & Haenni, 1997). Two sites for molecules binding: ADP site and NCB site were defined (Gupta et al., 2020). Here, three phenolic compounds were chosen as ligands for each binding site. Ritonavir (-9.4 kcal/mol) and Ivermectin (-9,7 kcal/mol) are respectively the drug's bending energy scores for ADP and NCP site. As shown in **Figure 2-A**, Tannins, biflavones, flavonol glycosides are the most ranked ligands with SARS-CoV 2 Helicase.

ADP site docking revealed that amentoflavone (-9 kcal/mol), dieckol (-9 kcal/mol), bilobetin (-8.9 kcal/mol) were the most efficient ligands (**Table 1**). Until the time of writing this work, any docking model has not yet evaluated these molecules. The present results reveal that the ADP site interacts with amentoflavone by 3 HB; Asp534 (A): 3.72Å, Glu375 (A): 3.11Å, Glu375 (A): 3.15Å and 11 HI; Ala316 (A), Glu540 (A), Gly538 (A), Ser289 (A), Ala313 (A), Gln537 (A), Lys288 (A), Asp374 (A), Met378 (A), Ser535 (A), Ala312 (A). Dieckol formed 4 HB; Arg443(A): 3.21Å, Lys320(A): 3.02Å, Ala316(A) 2.89 Å, Glu375(A): 3.05Å and 14 HI; Thr286(A), Gly285(A), Glu540(A), Arg442(A), Glu319(A), Ser539(A), Leu317(A), Gly538(A), Gln537(A), Ala312(A), Ala313(A), lys288(A), Asp374(A), Ser289(A). Bilobetin interacts with the ADP site by 2 HB; Glu540 (A): 2.86Å, Thr286 (A): 3.25Å and 10 HI; Ala316 (A), Gly538 (A), Ser289 (A), Ala312 (A), Gln537 (A), Lys288 (A), Asp374 (A), Glu375 (A), Glu319 (A), Ala313 (A) (**Figure 3**).

Consistent report (Jia et al., 2019) demonstrated that the helicase NTPase activity exist in a split located between 1A and 2A motor domains and made by the following 6 amino acids; Arg567, Gln404, Glu375, Asp374, Ser289 and Lys288. Four basic amino acid residues (Arg337, Arg339, Lys345 and Lys347) located at the top of nucleic acid binding channel are critical for reducing helicase activity.

Four of Amentoflavone complex residues are conformed by this study, which means that our docking model can reveal a valid therapeutic approach. The nucleic acids binding site

(NCB site) of helicase has more interesting binding energy scores than ADP site. The top three ranked molecules are Punigalagin, Tellimagrandin I and tannic acid with -10.9, -10.9 and -10.8 kcal/mol respectively. All these molecules are derivatives of natural tannins class, they are characterized by their high ability to reach a stable cross-linked association within different proteins by forming hydrogen bonding interaction (Fraga-Corral et al., 2020). Results in **Figure 3** show that the best ranked hydrolysable tannins are pedunculagin, where it interact by 11 hydrogen bonds with SARS-CoV-2 Helicase (Nsp13) residues; Thr380(A): 2.34Å, Asn361(A): 2.78Å, Lys139(A): 2.72Å, Glu197(A): 2.76Å, Arg337(A): 2.93Å, Arg337(A): 3.13Å, Thr288(A): 2.93Å, His230(A): 2.98Å, Lys149(A): 2.98Å, Pro408(A): 2.85Å, Met378(A): 3.31Å. In addition, pedunculagin is stabilized within the NCP site pocket with 10 hydrophobic interactions, Asp383(A), Cys309(A), Arg339(A), Ala338(A), The214(A), Val181(A), Asn179(A), glu142(A), Thr410(A), Try382(A). The pedunculagin / Helicase interaction has not been studied by subsequent work, through molecular docking analyses, a recent study shows that pedunculagin are the best hydrolysable tannins that can interact with the catalytic site SARS-CoV-2-3CL^{pro} residu (Khalifa et al., 2020). Tito et al. (2020) suggested that a pomegranate peel extract, containing 182.31 mg Pedunculagin /g of dried peels powder, can inhibit the the 3CL protease activity until 80%, reduce the Angiotensin-converting enzyme 2 and Transmembrane protease serine 2 precursor gene expression level by 30% and 70% respectively and inhibit the interaction between S protein and Angiotensin-converting enzyme 2 until 74%. Another structurally similar molecule, Tellimargrandin I which is found widely in *Cornus canadensis* (Lavoie et al., 2017), *Rosae Rugosae* (Tamura et al., 2010) and *Eucalyptus globulus* (Boulekbache-Makhlouf et al., 2010) plants, was reviewed by Zheng et al. (2012) for its wide spectra of biological activities. Here, it recorded a binding score energy of -10.9 kcal/mol, This molecule was reported to form a large H bond network with Lys146(A): 2.88Å, Asn361(A): 3.08Å, Thr410(A): 3.03Å, Pro408(A): 3.07Å, Pro408(A): 3.07Å, Thr380(A): 3.01Å, Asp383(A): 3.12Å, Met378(A): 2.69Å, Met378(A): 3.11Å, Arg178(A): 3.07Å, His311(A): 3.07Å, Asp315(A): 2.96Å, Arg339(A): 3.13Å, Arg339(A): 2.94Å, His230(A): 2.68Å, Thr288(A): 3.32Å, Thr288(A): 3.16Å, Thr288(A): 2.75Å. Also, it ensure the binding mode by the intraction through 10 HI; tur180(A), Asn179(A), Glu142(A), Lys139(A), Alu407(A), Ala379(A), Ser310(A), Cys309(A), Val181(A), Leu227(A) (**Figure 3**). In related work, Puttaswamy et al. (2020) reported that Tellimargrandin I showed its ability of a robust interaction with Spike protein (-8.1 kcal/mol), RdRp (-9.5 kcal/mol), TMPRSS2 (-8.6 kcal/mol). Tannic acid is the third best ligand recording a binding score energy of -10,8 kcal/mol, it can realize 16 hydrogen bonds; Glu375(A): 2.75Å, Asn179(A): 3.07Å, Arg179(A): 3.01Å, Arg339(A): 2.89Å, Arg339(A): 2.87Å, Ala336(A): 3.05Å, Ala336(A): 3.07Å, Lys139(A): 3.25Å, Lys139(A): 3.25Å, Asn361(A): 2.88Å, Asn361(A): 2.91Å, His230(A): 2.83Å, Val181(A): 3.01Å, Val181(A): 3.26Å,

Pro408(A): 3.10Å, Thr410(A): 3.11Å, and 13 hydrophobic interactions; Gln537(A), Ala312(A), Ala313(A), Asp534(A), Met378(A), Cys309(A), Thr199(A), Arg337(A), Gln197(A), Pro335(A), Thr380(A), Gln142(A), Leu138(A), Tyr382(A), VAl360(A), Lys146(A), Asp383(A), Tyr18(A) (**Figure 3**). Tannic acid is polyphenolic compound with high molecular weight, highly soluble in water. shown to possess antioxidant (Gülçin et al., 2010), antimutagenic (S.C. Chen & Chung, 2000) and anticarcinogenic properties (Baer-Dubowska et al., 2020). It has been stated to present the activity against Influenza A virus, Papilloma viruses, noroviruses, Herpes simplex virus type 1 and 2, and human immunodeficiency virus (HIV) (Kaczmarek, 2020). Moreover, in 2005, C.N. Chen et al. (2005) reported in *in vitro* study that tannic acid, was the potent molecule to inhibit the SARS-CoV-2 3CL^{pro} with high activity expressed by a low IC$_{50}$ value (3 μM).

Wenn diagram (**Figure 5**) summarizes the intersection between catalytic residues interactions. Ala316 (A), Glu540 (A), Gly538 (A), Ser289 (A), Ala313 (A), Gln537 (A), Asp374 (A), Ala312 (A) for Helicase (ADP site), Thr380(A), Asn361(A), Lys139 (A), His230 (A), Pro408 (A), Met378 (A), Asp383 (A), Cys309 (A), Arg339 (A), Val181 (A), Asn179 (A) and Thr410 (A) represent the common amino acids for Helicase (NCP site). All the residues were confirmed with amino acid listed in Helicase active site (**Table S2**, Appendix A supplementary data), leading us to conclude that these complexes are made in the right way. Ramachandran Plot (**Figure 4**) distributes the highly preferred observations, revealing that the protein stereochemistry is not affected by ligands/enzymes interaction, which confirms that these complexes are stable and robust. Taken together the obtained results, we can conclude that Helicase could be considered as a prospective target for covid virus inhibitors.

3.2.4   *RNA-dependent RNA polymerase (RdRP*

According to docking results (**Table S1**, Appendix A supplementary data), for RNA site the most binding energy scores were recorded for biflavone, flavonol glycoside, Tannins classes. Eight phenolic compounds have a scores superior to Ritonavir one used as a target control (Score Value: -9.5 kcal/mol). The top three compounds ranked against RNA site (Tannic acid, punicalagin, dieckol) were compiled in **Table 1**. Concerning RdRp (RTP site), Rupintrivir (-10,8 kcal/mol) was used as a target control, 13 phenolic compounds have a scores superior to this control. The top three ranked compounds against RdRp (RTP site); Dieckol, Chebulagic acid and tannic acid, were compiled in **Table 1**.

As for the SARS-CoV-2 RdRp (RNA site), Pedunculagin was recorded as the best ligand among 156 tested phenolic compounds against SARS-CoV-2 RdRp (RNA site). The origin and well-made of Punicalagin are already cited in helicase section, Binding interactions of the native ligand (binding score = -10.8 kcal/mol). As shown in **Figure 3,** there are 11 hydrogen bonds with Arg555(A): 2.85Å, Arg553(A): 3.16Å, Arg553(A): 3.11Å, Arg553(A): 2.94Å, Lys798(A):

3.08Å, Lys551(A): 3.15Å, Tyr621(A): 2.93Å, Tyr621(A): 2.73Å, Asn691(A): 3.06Å, Thr556(A): 3.03Å, Thr556(A): 2.77Å. Additionally, other interactions were observed with Pro620(A), Lys621(A), Asp618(A), Asp623(A), Cys622(A), Asp760(A), Thr687(A), Ser682(A), Lys545(A). The second ranked ligand is tannic acid (binding score = -10,6 kcal/mol) with 32 ligand/protein interactions (**Figure 3**); 20 of them were hydrogen bonds, Arg553(A): 2.91Å, Arg553(A): 2.83Å, Thr556(A): 2.77Å, Thr556(A): 3.03Å, Thr556(A): 2.80Å, Lys798(A): 3.00Å, Ser682(A): 3.16Å, Lys676(A): 3.00Å, The680(A): 2.87Å, Arg555(A): 2.96Å, Ser814(A): 2.84Å, Trp617(A): 2.90Å, Ser759(A): 2.69Å, Asp760(A): 2.88Å, Asp760(A): 3.28Å, Tyr619(A): 2.73Å, Lys621(A): 2.94Å, Asp618(A): 3.01Å, Asp618(A): 2.78Å, Asp618(A): 2.82Å, and 12 Hydrophobic interactions, Arg836(A), Cys622(A), Tyr456(A), Asp623(A), Lys551(A), Ala558(A), Val557(A), Ser681(A), Met542(A), Asp761(A), Cys813(A), Glu811(A). As described before, Dieckol is a major marine polyphenol reported for its wide antiviral activity, exhibited a docking score of -10.1 kcal/mol. Ligand interaction analysis of the Dieckol /RdRp (**Figure 3**) complex shows that ligand mostly made 7 hydrogen bonds; Tyr456(A): 2.79Å, Asp684(A): 3.11Å, Ala685(A): 3.20Å, Tyr689(A): 3.02Å, Gln573(A): 2.97Å, Arg569(A): 3.17Å, Asn497(A): 3.03Å and 10 hydrophobic interactions; Thr556(A), Thr680(A), Ala688(A), Leu576(A), Lys500(A), Thr687(A), Asp623(A), Ser682(A), Arg624(A), Ser681(A). The three ligands studied in this section are tannins, this result leads us to investigate the ability of this phenolic class to inhibit RNA dependent RNA polymerase. Wenn diagram summarizes the intersection between residues interactions, (**Figure 5**), Thr556 (A), Asp623 (A), Ser682 (A) were the common residue. Moreover, these amino acids were listed in the (**Table S 2**Appendix A supplementary data) and cited as interactive residue in several works (Ahmad et al., 2020), in SARS-CoV-2 RNA Dependent RNA polymerase (RdRp) docking study, Ahmad et al. (2020) Ahmad et al. (2020) showed that Thr556, Asp623 appear among the amino acids that interact with Carbetocin and Ser682 with Colistin, Demoxytocin and Lanreotide, with an interesting docking score. Further, 3-O-alpha-L-arabinopyranosyl-echinocystic acid and Genkwanin 8-C-beta-glucopyranoside were reported as potent RNA-Dependent RNA-Polymerase inhibitors involving Thr556 and Asp623 as hydrogen bonding residues (Khan et al., 2020). According to the obtained results, it could be concluded that probably the trio Thr556 (A), Asp623 (A), Ser682 (A) can be a catalytic triad for RNA-Dependent RNA-Polymerase. The binding mode stability was approved by the comparison of the backbone conformation of native SARS-COV-2 enzyme and the different molecules. Ramachandran plot showed that the residues were present in the favoured regions and the protein structure remains intact even in complex with the three molecules.

For the RdRp (RTP site), Rupintrivir was the best FDA-approved antiviral drug with binding score -10.8 kcal/mol, 15 phenolic compounds were found having superior scores. The major part of these molecules were tannins, biflavones,

flavanone glycosides, flavan-3-ols and flavonolignans. The top-ranked ligands are summarized in **Table 1**. Dieckol had the lowest binding energy score, -12.6 kcal/mol. The molecules were found to have 21 interactions (**Figure 3**); 3 HB with native RdRp (Ser759(A) 3.30Å, Arg836(A) 2.99Å and 3.08Å), 5 HB with RNA (u10(T) 3.01 and 3.03Å, a19(P) 3.05Å, u20(P) 3.07 and 2.69Å), 11 HI were also recorded, 2 with RNA (a11(T), U18(P)) and 9 with RdRp residues (Ala688(A), Thr687(A), Asn691(A), Val557(A), Ala547(A), Ile548(A), Asp845(A), Arg858(A), Arg555(A), Lys545(A)). The second ranked ligand is Chebulagic acid, it is a benzopyran tannin found in *Terminalia chebula* (Han et al., 2006), It has been proved to be immunosuppressive (Hamada et al., 1997), antitumor agent (Wang et al., 2018), hepatoprotective (Kinoshita et al., 2007), and alpha-glucosidase inhibitor (Sasidharan et al., 2012). In 2011, Lin et al. (2011) identified chebulagic acid and punicalagin, two hydrolysable tannins from fruits of *Terminalia chebula* Retz, which exhibit their antiviral activities by targeting HSV-1 viral glycoproteins that interact with cell surface heparin sulphate. In 2013, Lin et al. (2013) confirmed the antiviral activity of these tannin by exploring the antiviral potential of these two tannins against several viruses that use glycosaminoglycans for entry. The ligplot results (**Figure 3)** show that this chebulagic acid interacts with RdRp with 17 hydrogen bonds; 12 HB with native RdRp (Asn691(A): 3.33Å, Ser759(A): 3.23Å, Ser759(A) : 3.11Å, Arg553(A) : 2.97Å, His439(A) : 3.13Å, Arg836(A) : 3.19Å, Arg836(A) : 2.98Å, Arg836(A) : 3.07Å, Thr556(A) : 2.78Å, Thr556(A) : 2.70Å), 2 HB bonded to magnesium of the protein (Tyr619(A) 3.34Å and Asp760(A) 3.17Å) and 5 HB with RNA (u20(P) 3.06Å, u20(P) 3.11Å, u20(P) 2.95Å, a19(P) 2.84Å). Furthermore, this compound formed a hydrophobic interactions network with the surrounding amino acid, including 11 residues Val557 (A), Asp623 (A), Arg555 (A), Ile548 (A), Ser549 (A) and Asp618 (A). Tannic acid is the third best ligand with -11.7 kcal/mol, it can realize 28 HB and 13 HI, as for chebulagic acid, the hydrogen bonds are distributed in three categories: 11 RNA/ ligands, 11 RdRp/ ligands and six RdRp/ magnesium /ligands. The 11 RNA/ ligands are reported with u20(P), u10(T) and u18(P) having different distances, u20(P): 2.33Å, 3.03Å, 3.13Å,2.90Å, 2.82Å, 2.74Å, u10(T): 2.85Å, 2.85Å, 3.02Å and u18(P) 2.78Å, 2.98Å, the 11 RdRp/ ligands are Asn691(A) 3.03Å, Ser759(A) 2.70Å, Cys622(A) 3.06Å, Lys545(A) 3.11Å, Lys545(A) 3.04Å, Lys545(A) 2.92Å, Ser814(A) 2.81Å, Asp623(A) 2.68Å, Arg553(A) 2.76Å, Arg836(A) 2.94Å, Ser682(A) 2.92Å. The 6 RdRp/ magnesium/ligands are Asp761(A): 2.33/mg101(P)/3.08, Asp761(A): 2.63/mg101(P)/3.08, Trp800(A): 3.18/mg1005(A)/2.38, Glu811(A): 3.09/mg1005(A)/2.66, Tyr619(A): 3.34/mg1004(A)/2.61, Asp760(A): 3.17/mg1004(A)/3.19. Moreover, Tannic acid is stabilized by 13 HI, Lys551(A), Ala550(A), Arg555(A), Thr556(A), Thr687(A), Val557(A), Ala688(A), Lys621(A), Cys813(A), Asp618(A) with RdRp and a11(T), u17(P), a19(P) with RNA (**Figure 3**). This mass of interactions is explained by the fact that tannic acid has many hydroxyl groups and a

very variable geometric structure. Wenn diagram (**Figure 5**) summarizes common residues and nucleotides. It was found that the three ligands interact with u20 (P), a19 (P) from the RNA nucleotides and with Asn691 (A), Ser759 (A), Arg836 (A), Val557 (A), Arg555 (A) from the RdRp residues. These findings are in agreement with the work of Singh et al. (2020) who revealed that Remdesivir (an FDA-approved intravenous antiviral drug) characterized by HB interaction with u20 from RNA nucleotides and having a binding pocket residue including Arg553, Arg555, Thr556 and Asn691, explaining its potential inhibitory effect. Moreover, Bastikar et al. (2020) confirmed that the docking of curcumin and allicin derivatives with RdRp exhibited notale binding affinity and having interactions with U10, A11 and U20 nucleotides and amino acid residues such as Asp623, Asn691, Arg555 and Ser682 which are highly involved in the HB with most of the tested ligands. Ramachandran Plot (**Figure 5**) distribute the highly preferred observations, which revealed that the protein stereochemistry is not affected by ligands/enzymes interaction, thus it is confirmed that these complexes are stable and robust.

From the obtained results, we can conclude that the molecular docking analysis could be a good tool for virtual screening and preliminary step towards searching for effective drugs against selected targeted protein/ enzyme.

3.3. Drug-likeness

Pharmacophore modelling to identify drug-like compounds is a common tool for in silico drug identification (Yang, 2010) by Drug-likeness analysis. SwissADME is a tool provided by the Swiss institute of Bioinformatics (Daina et al., 2017), used to predict physiochemical properties, lipophilicity, water-solubility, pharmacokinetics, drug-likeness and medicinal Chemistry. According the results of drug-likeness analysis predictions all the studied phenolic compounds have small bioavailability score. The Abbott bioavailability score (ABS) determines whether it passes or violates Lipinski's rule of five. Generally, a molecule is estimated to have more than 10% of bioavailability (F) in case it passes Lipinski's rule of five with ABS of 0.55 in pH constant conditions (Martin, 2005).

In current study, Chebulagic acid has reduced bioavailability (ABS: 0.11), Amentoflavone, Dieckol, Punicalagin, Tellimagrandin I, Tannic acid and Punicalagin recorded a bit higher score (ABS: 0.17), Bilobetin, Sciadopitysin, Ginkgetin revealed a relative high bioavailability (ABS: 0.55). Nevertheless, their bioavailability score makes them ineffectual via oral route. Similar results are recorded with FDA SARS-Cov-2 recognized drugs, they varied from 0.17 to 0.56 (**Table S3**Appendix A supplementary data). Lipinski's rule of 5 provides an overview of the drug-like inhibitor candidate (Lipinski et al., 1997). In general, phenolic compounds presenting a violation value higher than 1 do not meet the criteria for drug-likeness (MW less than 500, cLogP less than 5, number of hydrogen-bond acceptors (HBA) less than 10 and number of hydrogen-bond donors (HBD) less than 5). In fact, the study of our phenolic compounds shows only 3 candidates with one violation:

Bilobetin, Sciadopitysin and Ginkgetin. The rest of molecules exhibited a higher MV than that proposed by Lipinski, but it is crucial to note that Ivermectin, Lopinavir, Remdesivir, Ritonavir, Rupintrivir, Tipranavir, the most probable drugs according clinical studies, present similar MW :875.09, 628.80, 602.58, 720.94, 598.66, 602.66 DA respectively (**Table 2**). Furthermore, according to Veber's rules (Veber et al., 2002), satisfactory bioavailability is more suitable for compounds with ≤ 10 rotatable bonds (RB) and topological polar surface area (TPSA) ≤ 140 Å^2. Considering these rules, the predicted proprieties point to that among nine drug-like inhibitor candidates, 8 compounds with TPSA > 140 Å^2 fulfill the Veber's rules and only Tannic acid with 31 RB do not fulfill the rules. PAINS (Pan Assay Interference Compounds) (Baell & Holloway, 2010) evaluation revealed that only Amentoflavone, Dieckol, Bilobetin, Sciadopitysin and Ginkgetin do not present any PAINS alert. Punicalagin, Tellimagrandin I, Tannic acid and Chebulagic acid present one alert, this distribution is a function of chemical class. In fact, biflavones do not present any resemblance to PAINS, but tannins can be classified as PAINS. This tendency is also observed with another medicinal chemistry model, biflavones were not determined to have any Brenk fragments (Brenk et al., 2008). Similar trend has been proved by previous study (Sayed et al., 2020), in which authors confirm that biflavones mainly amentoflavone have an efficient drug-like properties, based on their pharmacokinetics parameters (e.g., absorption and bioavailability), and Lipinski's rules of 5 obedience (**Table 2**).

4. CONCLUSION

Taken together all the attained results, we can concluded that the screening of 9900 ligands / SARS-Cov-2 Proteins complex through docking analysis is a promising way to identify possibly effective drugs against COVID-19. By studying the interactions of 33 phenolic classes with six viral vital enzymes (Main protease, Papain-like protease, Helicase (ADP and NCP sites) and RNA-dependent RNA polymerase (RNA and RTP sites)). biflavone and tannin classes present an important binding energy score. Further investigation shows that a range of 156 drug candidates was tiered according to their binding energy scores for each protein. The top three ranked phenolic compounds were subject of residue/molecules moieties interaction analyses. The interaction results revealed that the active sites of each enzyme were conserved with three common residues at least. The stereochemistry of complexes analysed by Ramachandran plot proved that ligands pose do not affect the native enzyme structure. The section of docking screening gave nine phenolic compounds as a potential SARS-Cov-2 inhibitor which are classified as following: 4 biflavones (Amentoflavone, Sciadopitysin, Bilobetin, Ginkgetin and Dieckol) and 5 tannins (Punicalagin, Tellimagrandin I, Tannic acid and Chebulagic acid). A Drug-likeness analysis was realized to evaluate the ability of these candidates to be a recognized as drugs against covid-19. Only the flavone class shows efficiency by one violation of Lipinski's rules of five, which in turn is consistent

with similar results observed for medicinal chemistry by PAINS and Brenk models. Clearly, all observations of this study point to a further required works in order to examine deeply the possibility of using these molecules, which could be subjected for several pre-clinical studies.

CONFLICTS OF INTEREST

The authors declare no conflict of interest.

ORCID

Hammami Majdi   0000-0002-4376-0638

Feten Zar Kalai   0000-0001-6460-8777

Walid Yeddes   0000-0002-1439-7956

Moufida Saidani   0000-0001-6052-1367

A. APPENDIX. SUPPLEMENTARY DATA

Supplementary data to this article can be found online at https://doi.org/10.53365/nrfhh/143085

AUTHOR CONTRIBUTIONS

HM, FZK, WY - Research concept and design, HM, FZK, WY - Collection and/or assembly of data, HM, FZK, WY - Data analysis and interpretation, HM, FZK, WY - Writing the article, HM, FZK, WY - Critical revision of the article, MS - Final approval of the article.

REFERENCES

Abdillah, S., Cita, Y.P., 2020. Potential target plants as anti-sars-cov-2 (Coronavirus): Expectations and challenges. Indian journal of pharmacy and pharmacology. 7, 57–65. https://doi.org/10.18231/j.ijpp.2020.013

Adnan, M., Rasul, A., Hussain, G., Shah, M.A., Zahoor, M.K., Anwar, H., Sarfraz, I., Riaz, A., Manzoor, M., Adem, Ş., 2020. Ginkgetin: A natural biflavone with versatile pharmacological activities. Food and Chemical Toxicology. 145, 111642. https://doi.org/10.1016/j.fct.2020.111642

Ahmad, J., Ikram, S., Ahmad, F., Rehman, I.U., Mushtaq, M., 2020. SARS-CoV-2 RNA Dependent RNA polymerase (RdRp)-A drug repurposing study. Heliyon. 6, 4502–4502. https://doi.org/10.1016/j.heliyon.2020.e04502

Alamri, M.A., Qamar, M.T., Mirza, M.U., Alqahtani, S.M., Froeyen, M., Chen, L.L., 2020. Discovery of human coronaviruses pan-papain-like protease inhibitors using computational approaches. Journal of Pharmaceutical Analysis. 10, 546–559. https://doi.org/10.1016/j.jpha.2020.08.012

Andersen, K.G., Rambaut, A., Lipkin, W.I., Holmes, E.C., Garry, R.F., 2020. The proximal origin of SARS-CoV-2. Nature Medicine. 26, 450–452. https://doi.org/10.1038/s41591-020-0820-9

Augustin, T.L., Hajbabaie, R., Harper, M.T., Rahman, T., 2020. Novel Small-Molecule Scaffolds as Candidates against the SARS Coronavirus 2 Main Protease: A Fragment-Guided in Silico Approach. Molecules. 25, 5501. https://doi.org/10.3390/molecules25235501

Baell, J.B., Holloway, G.A., 2010. New substructure filters for removal of pan assay interference compounds (PAINS) from screening libraries and for their exclusion in bioassays. Journal of medicinal chemistry. 53, 2719–2740. https://doi.org/10.1021/jm901137j

Baer-Dubowska, W., Szaefer, H., Majchrzak-Celińska, A., Krajka-Kuźniak, V., 2020. Tannic acid: specific form of tannins in cancer chemoprevention and therapy-old and new applications. Current Pharmacology Reports. 6, 28–37. https://doi.org/10.1007/s40495-020-00211-y

Banerjee, T., Valacchi, G., Ziboh, V.A., Van Der, Vliet, A., 2002. Inhibition of TNFα-induced cyclooxygenase-2 expression by amentoflavone through suppression of NF-κB activation in A549 cells. Molecular Cellular Biochemistry. 238, 105–110. https://doi.org/10.1023/a:1019963222510

Bastikar, V.A., Bastikar, A.V., Chhajed, S.S., 2020. Understanding the Role of Natural Medicinal Compounds Such as Curcumin and Allicin against SARS-CoV-2 Proteins as Potential Treatment against COVID-19: An In silico Approach. Journal of Proteomics & Bioinformatics. 13, 1–14.

Bobrowski, T., Alves, V., Melo-Filho, C.C., Korn, D., Auerbach, S., Schmitt, C., Muratov, E., Tropsha, A., 2020. Computational models identify several FDA approved or experimental drugs as putative agents against SARS-CoV-2. ChemRxiv . https://doi.org/10.26434/chemrxiv.12153594

Boulekbache-Makhlouf, L., Meudec, E., Chibane, M., Mazauric, J.P., Slimani, S., Henry, M., Cheynier, V., Madani, K.J., 2010. Analysis by high-performance liquid chromatography diode array detection mass spectrometry of phenolic compounds in fruit of Eucalyptus globulus cultivated in Algeria. Journal of Agricultural Food Chemistry. 58, 12615–12624. https://doi.org/10.1021/jf1029509

Brenk, R., Schipani, A., James, D., Krasowski, A., Gilbert, I.H., Frearson, J., Wyatt, P.G., 2008. Lessons learnt from assembling screening libraries for drug discovery for neglected diseases. ChemMedChem. 3, 435–435. https://doi.org/10.1002/cmdc.200700139

Chauhan, S., 2020. Comprehensive review of coronavirus disease 2019 (COVID-19). Biomedical Journal. 43, 334–340. https://doi.org/10.1016/j.bj.2020.05.023

Chen, C.N., Lin, C.P., Huang, K.K., Chen, W.C., Hsieh, H.P., Liang, P.H., Hsu, J.T., A, ., 2005. Inhibition of SARS-CoV 3C-like Protease Activity by Theaflavin-3,3'-digallate (TF3). Evidence-Based Complementary and Alternative Medicine. 2, 209–215. https://doi.org/10.1093/ecam/neh081

Chen, F., Chan, K., Jiang, Y., Kao, R., Lu, H., Fan, K., Cheng, V., Tsui, W., Hung, I., Lee, T., 2004. In vitro susceptibility of 10 clinical isolates of SARS coronavirus to selected antiviral compounds. Journal of Clinical Virology. 31, 69–75. https://doi.org/10.1016/j.jcv.2004.03.003

Chen, S.C., Chung, K.T., 2000. Mutagenicity and antimutagenicity studies of tannic acid and its related compounds. Food and Chemical Toxicology. 38, 1–5. https://doi.org/10.1016/s0278-6915(99)00114-3

Choi, J.S., Lee, K., Lee, B.B., Kim, Y.C., Kim, Y.D., Hong, Y.K., Cho, K.K., Choi, I.S., 2014. Antibacterial activity of the phlorotannins dieckol and phlorofucofuroeckol-A from Ecklonia cava against Propionibacterium acnes. Botanical Sciences. 92, 425–431.

Choi, S.K., Oh, H.M., Lee, S.K., Jeong, D.G., Ryu, S.E., Son, K.H., Han, D.C., Sung, N.D., Baek, N.I., 2006. Biflavonoids inhibited phosphatase of regenerating liver-3 (PRL-3). Natural product research. 20, 341–346. https://doi.org/10.1080/14786410500463312

Daina, A., Michielin, O., Zoete, V., 2017. SwissADME: a free web tool to evaluate pharmacokinetics, drug-likeness and medicinal chemistry friendliness of small molecules. Scientific Reports. 7, 42717–42717. https://doi.org/10.1038/srep42717

Demšar, J., Curk, T., Erjavec, A., Č Gorup, Hočevar, T., Milutinovič, M., Možina, M., Polajnar, M., Toplak, M., Starič, A., 2013. Orange: data mining toolbox in Python. the Journal of machine Learning research.

14, 2349–2353.

Egan, W.J., Merz, K.M., Baldwin, J.J.J.J., 2000. Prediction of drug absorption using multivariate statistics. Journal of Medicinal Chemistry. 43, 3867–3877. https://doi.org/10.1021/jm000292e

Eom, S.H., Moon, S.Y., Lee, D.S., Kim, H.J., Park, K., Lee, E.W., Kim, T.H., Chung, Y.H., Lee, M.S., Kim, Y.M., 2015. In vitro antiviral activity of dieckol and phlorofucofuroeckol-A isolated from edible brown alga Eisenia bicyclis against murine norovirus. Algae. 30, 241–246. https://doi.org/10.4490/algae.2015.30.3.241

Estrada, E.J., 2020. Topological analysis of SARS CoV-2 main protease. Chaos. 30, 61102–61102. https://doi.org/10.1063/5.0013029

Fraga-Corral, M., García-Oliveira, P., Pereira, A.G., Lourenço-Lopes, C., Jimenez-Lopez, C., Prieto, M.A., Simal-Gandara, J., 2020. Technological application of tannin-based extracts. Molecules. 25, 614. https://doi.org/10.3390/molecules25030614

Freitas, A., Almeida, M., Andrighetti-Fröhner, C., Cardozo, F., Barardi, C., Farias, M., Simões, C., 2009. Antiviral activity-guided fractionation from Araucaria angustifolia leaves extract. Journal of Ethnopharmacology. 126, 512–517. https://doi.org/10.1016/j.jep.2009.09.005

Gentile, D., Patamia, V., Scala, A., Sciortino, M.T., Piperno, A., Rescifina, A., 2020. Putative inhibitors of SARS-CoV-2 main protease from a library of marine natural products: A virtual screening and molecular modeling study. Marine Drugs. 18, 225. https://doi.org/10.3390/md18040225

Ghose, A.K., Viswanadhan, V.N., Wendoloski, J.J., 1999. A knowledge-based approach in designing combinatorial or medicinal chemistry libraries for drug discovery. 1. A qualitative and quantitative characterization of known drug databases. Journal of Combinatorial Chemistry. 1, 55–68. https://doi.org/10.1021/cc9800071

Ghosh, R., Chakraborty, A., Biswas, A., Chowdhuri, S., 2020. Computer aided identification of potential SARS CoV-2 main protease inhibitors from diterpenoids and biflavonoids of Torreya nucifera leaves. Journal of Biomolecular Structure Dynamics, 1–16. https://doi.org/10.1080/07391102.2020.1841680

Gu, Q., Li, Y., Chen, Y., Yao, P., Ou, T.J.N., 2013. Sciadopitysin: active component from Taxus chinensis for anti-Alzheimer's disease. Natural Product Research. 27, 2157–2160. https://doi.org/10.1080/14786419.2013.790031

Guinea, M., Franco, V., Araujo-Bazán, L., Rodríguez-Martín, I., González, S., 2012. In vivo UVB-photoprotective activity of extracts from commercial marine macroalgae. Food and Chemical Toxicology. 50, 1109–1117. https://doi.org/10.1016/j.fct.2012.01.004

Gülçin, İ., Huyut, Z., Elmastaş, M., Aboul-Enein, H.Y., 2010. Radical scavenging and antioxidant activity of tannic acid. Arabian Journal of Chemistry. 3, 43–53. https://doi.org/10.1016/j.arabjc.2009.12.008

Gupta, S., Biswal, P.S., Panda, S., Ray, S.K., Rana, A.K., K, M., 2020. Binding mechanism and structural insights into the identified protein target of COVID-19 and importin-α with in-vitro effective drug ivermectin. Journal of Biomolecular Structure Dynamics, 1–10. https://doi.org/10.1080/07391102.2020.1839564

Hamada, S., Kataoka, T., Woo, J.T., Yamada, A., Yoshida, T., Nishimura, T., Otake, N., Nagai, K., 1997. Immunosuppressive effects of gallic acid and chebulagic acid on CTL-mediated cytotoxicity. Biological Pharmaceutical Bulletin. 20, 1017–1019. https://doi.org/10.1248/bpb.20.1017

Han, Q., Song, J., Qiao, C., Wong, L., Xu, H., 2006. Preparative isolation of hydrolysable tannins chebulagic acid and chebulinic acid from Terminalia chebula by high-speed counter-current chromatography. Journal of Separation Science. 29, 1653–1657. https://doi.org/10.1002/jssc.200600089

Hui, D.S., Azhar, E.I., Madani, T.A., Ntoumi, F., Kock, R., Dar, O.,

Ippolito, G., Mchugh, T.D., Memish, Z.A., Drosten, C., 2020. The continuing 2019-nCoV epidemic threat of novel coronaviruses to global health-The latest 2019 novel coronavirus outbreak in Wuhan, China. International Journal of Infectious Diseases. 91, 264–266. https://doi.org/10.1016/j.ijid.2020.01.009

Islam, M.R., Hoque, M.N., Rahman, M.S., Alam, A.R.U., Akther, M., Puspo, J.A., Akter, S., Sultana, M., Crandall, K.A., Hossain, M.A., 2020. Genome-wide analysis of SARS-CoV-2 virus strains circulating worldwide implicates heterogeneity. Scientific reports. 10, 14004. https://doi.org/10.1038/s41598-020-70812-6

Jia, Z., Yan, L., Ren, Z., Wu, L., Wang, J., Guo, J., Zheng, L., Ming, Z., Zhang, L., Lou, Z., 2019. Delicate structural coordination of the Severe Acute Respiratory Syndrome coronavirus Nsp13 upon ATP hydrolysis. Nucleic Acids Research. 47, 6538–6550. https://doi.org/10.1093/nar/gkz409

Jin, Z., Du, X., Xu, Y., Deng, Y., Liu, M., Zhao, Y., Zhang, B., Li, X., Zhang, L., Peng, C.J.N., 2020. Structure of M pro from SARS-CoV-2 and discovery of its inhibitors. Nature Medicine. 582, 289–293. https://doi.org/10.1038/s41586-020-2223-y

Kaczmarek, B., 2020. Tannic acid with antiviral and antibacterial activity as a promising component of biomaterials-A minireview. Materials. 13, 3224. https://doi.org/10.3390/ma13143224

Kadaré, G., Haenni, A.L., 1997. Virus-encoded RNA helicases. Journal of Virology. 71. https://doi.org/10.1128/jvi.71.4.2583-2590.1997

Khalifa, I., Zhu, W., Mohammed, H.H.H., Dutta, K., Li, C., 2020. Tannins inhibit SARS-CoV-2 through binding with catalytic dyad residues of 3CLpro: An in silico approach with 19 structural different hydrolysable tannins. Journal of food biochemistry. 44, e13432. https://doi.org/10.1111/jfbc.13432

Khan, A., Khan, M., Saleem, S., Babar, Z., Ali, A., Khan, A.A., Sardar, Z., Hamayun, F., Ali, S.S., Wei, D.Q., 2020. Phylogenetic analysis and structural perspectives of RNA-dependent RNA-polymerase inhibition from SARs-CoV-2 with natural products. Interdisciplinary Sciences: Computational Life Sciences. 12, 335–348. https://doi.org/10.1007/s12539-020-00381-9

Kim, S., Thiessen, P.A., Bolton, E.E., Chen, J., Fu, G., Gindulyte, A., Han, L., He, J., He, S., Shoemaker, B.A., 2016. PubChem substance and compound databases. Nucleic Acids Research. 44, 1202–1213. https://doi.org/10.1093/nar/gkv951

Kinoshita, S., Inoue, Y., Nakama, S., Ichiba, T., Aniya, Y., 2007. Antioxidant and hepatoprotective actions of medicinal herb, Terminalia catappa L. from Okinawa Island and its tannin corilagin. Phytomedicine. 14, 755–762. https://doi.org/10.1016/j.phymed.2006.12.012

Koirala, P., Jung, H.A., Choi, J.S., 2017. Recent advances in pharmacological research on Ecklonia species: a review. Archives of Pharmacal Research. 40, 981–1005. https://doi.org/10.1007/s12272-017-0948-4

Kong, R., Yang, G., Xue, R., Liu, M., Wang, F., Hu, J., Guo, X., Chang, S., 2020. COVID-19 Docking Server: A meta server for docking small molecules, peptides and antibodies against potential targets of COVID-19. Bioinformatics. 36, 5109–5111. https://doi.org/10.1093/bioinformatics/btaa645

Krauze-Baranowska, M., Pobłocka, L., Helab, A.A.E., 2005. Biflavones from Chamaecyparis obtusa. Zeitschrift für Naturforschung C. 60, 679–685. https://doi.org/10.1515/znc-2005-9-1004

Krauze-Baranowska, M., Wiwart, M., 2003. Antifungal activity of biflavones from Taxus baccata and Ginkgo biloba. Zeitschrift für Naturforschung C. 58, 65–69. https://doi.org/10.1515/znc-2003-1-212

Lavoie, S., Côté, I., Pichette, A., Gauthier, C., Ouellet, M., Nagau-Lavoie, F., Mshvildadze, V., Legault, J., 2017. Chemical composition and anti-herpes simplex virus type 1 (HSV-1) activity of extracts from

Cornus canadensis. BMC Complementary Alternative Medicine. 17, 123–123. https://doi.org/10.1186/s12906-017-1618-2

Lee, S., Kim, J., Yoo, S., Kwon, S., 2013. Cytoprotective effect of dieckol on human endothelial progenitor cells (hEPCs) from oxidative stress-induced apoptosis. Free Radical Research. 47, 526–534. https://doi.org/10.3109/10715762.2013.797080

Li, F., Song, X., Su, G., Wang, Y., Wang, Z., Jia, J., Qing, S., Huang, L., Wang, Y., Zheng, K., 2019. Amentoflavone inhibits HSV-1 and ACV-resistant strain infection by suppressing viral early infection. Viruses. 11, 466–466. https://dx.doi.org/10.3390/v11050466

Li, M., Li, B., Hou, Y., Tian, Y., Chen, L., Liu, S., Zhang, N., Dong, J.J.P.R., 2019. Anti-inflammatory effects of chemical components from Ginkgo biloba L. male flowers on lipopolysaccharide-stimulated RAW264.7 macrophages. Phytotherapy Research. 33, 989–997. https://doi.org/10.1002/ptr.6292

Li, M., Li, B., Xia, Z.M., Tian, Y., Zhang, D., Rui, W.J., Dong, J.X., Xiao, F.J., 2219. Anticancer effects of five biflavonoids from Ginkgo Biloba L. male flowers in vitro. Molecules. 24, 1496. https://doi.org/10.3390/molecules24081496

Li, Y.L., Chen, X., Niu, S.Q., Zhou, H.Y., Li, Q.S., 2020. Protective Antioxidant Effects of Amentoflavone and Total Flavonoids from Hedyotis diffusa on H2O2-Induced HL-O2 Cells through ASK1/p38 MAPK Pathway. Chemistry & Biodiversity. 17, e2000251. https://doi.org/10.1002/cbdv.202000251

Lin, L.T., Chen, T.Y., Chung, C.Y., Noyce, R.S., Grindley, T.B., Mccormick, C., Lin, T.C., Wang, G.H., Lin, C.C., Richardson, C.D., 2011. Hydrolyzable tannins (chebulagic acid and punicalagin) target viral glycoprotein-glycosaminoglycan interactions to inhibit herpes simplex virus 1 entry and cell-to-cell spread. Journal of virology. 85, 4386–4398. https://doi.org/10.1128/jvi.01492-10

Lin, L.T., Chen, T.Y., Lin, S.C., Chung, C.Y., Lin, T.C., Wang, G.H., Anderson, R., Lin, C.C., Richardson, C.D., 2013. Broad-spectrum antiviral activity of chebulagic acid and punicalagin against viruses that use glycosaminoglycans for entry. BMC microbiology. 13, 187–187. https://doi.org/10.1186/1471-2180-13-187

Lipinski, C.A., Lombardo, F., Dominy, B.W., Feeney, P.J., 1997. Experimental and computational approaches to estimate solubility and permeability in drug discovery and development settings. Advanced Drug Delivery Reviews. 23, 3–25. https://doi.org/10.1016/S0169-409X(96)00423-1

Liu, P.K., Weng, Z.M., Ge, G.B., Li, H.L., Ding, L.L., Dai, Z.R., Hou, X.D., Leng, Y.H., Yu, Y., Hou, J., 2018. Biflavones from Ginkgo biloba as novel pancreatic lipase inhibitors: Inhibition potentials and mechanism. International Journal of Biological Macromolecules. 118, 2216–2223. https://doi.org/10.1016/j.ijbiomac.2018.07.085

Lobstein-Guth, A., Briancon-Scheid, F., Victoire, C., Haag-Berrurier, M., Anton, R., 1988. Isolation of amentoflavone from Ginkgo biloba. Planta medica. 54, 555–556. https://doi.org/10.1055/s-2006-962549

Lou, J.S., Bi, C., Chan, G., Dong, T., Tsim, K., 2017. Ginkgetin, a biflavonoid derived from leaves of Ginkgo biloba, induces autophagic cell death in non-small cell lung cancer via p62. Oncotarget. 8, 93131–93148. https://doi.org/10.18632/oncotarget.21862

Martin, Y.C., 2005. A bioavailability score. Journal of Medicinal Chemistry. 48, 3164–3170. https://doi.org/10.1021/jm0492002

Michler, H., Laakmann, G., Wagner, H., 2011. Development of an LC-MS method for simultaneous quantitation of amentoflavone and biapigenin, the minor and major biflavones from Hypericum perforatum L., in human plasma and its application to real blood. Phytochemical Analysis. 22, 42–50. https://doi.org/10.1002/pca.1249

Moon, H.E., Islam, M.N., Ahn, B.R., Chowdhury, S.S., Sohn, H.S., Jung, H.A., Choi, J.S., 2011. Protein tyrosine phosphatase 1B and α-glucosidase inhibitory phlorotannins from edible brown algae, Ecklonia stolonifera and Eisenia bicyclis. Bioscience, Biotechnology, and Biochemistry. 75, 1472–1480. https://doi.org/10.1271/bbb.110137

Muegge, I., Heald, S.L., Brittelli, D., 2001. Simple selection criteria for drug-like chemical matter. Journal of Medicinal Chemistry. 44, 1841–1846. https://doi.org/10.1021/jm015507e

Nukoolkarn, V., Lee, V.S., Malaisree, M., Aruksakulwong, O., Hannongbua, S., 2008. Molecular dynamic simulations analysis of ritronavir and lopinavir as SARS-CoV 3CLpro inhibitors. Journal of Theoretical Biology. 254, 861–867. https://doi.org/10.1016/j.jtbi.2008.07.030

Park, J.Y., Kim, J.H., Kwon, J.M., Kwon, H.J., Jeong, H.J., Kim, Y.M., Kim, D., Lee, W.S., Ryu, Y.B., 2013. Dieckol, a SARS-CoV 3CLpro inhibitor, isolated from the edible brown algae Ecklonia cava. Bioorganic & Medicinal Chemistry. 21, 3730–3737. https://doi.org/10.1016/j.bmc.2013.04.026

Puttaswamy, H., Gowtham, H.G., Ojha, M.D., Yadav, A., Choudhir, G., Raguraman, V., Kongkham, B., Selvaraju, K., Shareef, S., Gehlot, P., 2020. In silico studies evidenced the role of structurally diverse plant secondary metabolites in reducing SARS-CoV-2 pathogenesis. Scientific reports. 10, 20584. https://doi.org/10.1038/s41598-020-77602-0

Qamar, M.T.U., Alqahtani, S.M., Alamri, M.A., Chen, L.L., 2020. Structural basis of SARS-CoV-2 3CLpro and anti-COVID-19 drug discovery from medicinal plants. Journal of Pharmaceutical Analysis. 10(4), 313–319. https://doi.org/10.1016/j.jpha.2020.03.009

Ramaiah, R., Suresh, P.C., 2013. Molecular docking studies of phytochemical compounds with viral proteases. International Journal of Pharmaceutical Sciences Research. 4, 475–482. http://dx.doi.org/10.13040/IJPSR.0975-8232.4(1).475-82

Rameshkumar, M.R., Indu, P., Arunagirinathan, N., Venkatadri, B., El-Serehy, H.A., Ahmad, A., 2021. Computational selection of flavonoid compounds as inhibitors against SARS-CoV-2 main protease, RNA-dependent RNA polymerase and spike proteins: A molecular docking study. Saudi Journal of Biological Sciences. 28, 448–458. https://doi.org/10.1016/j.sjbs.2020.10.028

Rana, S., Sharma, S., Ghosh, K.S., 2020. Virtual screening of naturally occurring antiviral molecules for SARS-CoV-2 mitigation using docking tool on multiple molecular targets. ChemRxiv. Cambridge: Cambridge Open Engage, Pre-Print.

Ruan, X., Yan, L.Y., Li, X.X., Liu, B., Zhang, H., Wang, Q., 2014. Optimization of process parameters of extraction of amentoflavone, quercetin and ginkgetin from Taxus chinensis using supercritical CO2 plus co-solvent. Molecules. 19, 17682–17696. https://doi.org/10.3390/molecules191117682

Russo, M., Moccia, S., Spagnuolo, C., Tedesco, I., Russo, G.L., 2020. Roles of flavonoids against coronavirus infection. Chemico-Biological Interactions. 328, 109211. https://doi.org/10.1016/j.cbi.2020.109211

Rut, W., Lv, Z., Zmudzinski, M., Patchett, S., Nayak, D., Snipas, S.J., Oualid, F.E., Huang, T.T., Bekes, M., Drag, M., 2020. Activity profiling and crystal structures of inhibitor-bound SARS-CoV-2 papain-like protease: A framework for anti-COVID-19 drug design. Science Advances. 6(42), eabd4596. https://doi.org/10.1126/sciadv.abd4596

Ryu, Y.B., Jeong, H.J., Kim, J.H., Kim, Y.M., Park, J.Y., Kim, D., Naguyen, T.T.H., Park, S.J., Chang, J.S., Park, K.H.J.B., 2010. Biflavonoids from Torreya nucifera displaying SARS-CoV 3CLpro inhibition. Bioorganic & Medicinal Chemistry. 18, 7940–7947. https://doi.org/10.1016/j.bmc.2010.09.035

Ryu, Y.B., Jeong, H.J., Yoon, S.Y., Park, J.Y., Kim, Y.M., Park, S.J., Rho, M.C., Kim, S.J., Lee, W.S.J., 2011. Influenza virus neuraminidase inhibitory activity of phlorotannins from the edible brown alga Ecklonia cava. Journal of Agricultural and Food Chemistry. 59, 6467–6473. https://doi.org/10.1021/jf2007248

Sanjeewa, K.A., Fernando, I., Kim, H.S., Jayawardena, T.U., Ryu, B., Yang, H.W., Ahn, G., Lee, W., Jeon, Y.-J.J.J.O.A.P., 2020. Dieckol: an algal polyphenol attenuates urban fine dust-induced inflammation in RAW 264.7 cells via the activation of anti-inflammatory and antioxidant signaling pathways. Journal of Applied Phycology. 32, 2387–2396. https://doi.org/10.1007/s10811-019-01964-w

Sasidharan, I., Sundaresan, A., Nisha, V., Kirishna, M.S., Raghu, K., Jayamurthy, P., 2012. Inhibitory effect of Terminalia chebula Retz. fruit extracts on digestive enzyme related to diabetes and oxidative stress. Journal of Enzyme Inhibition Medicinal Chemistry. 27, 578–586. https://doi.org/10.3109/14756366.2011.603130

Sayed, A.M., Khattab, A.R., Aboulmagd, A.M., Hassan, H.M., Rateb, M.E., Zaid, H., Abdelmohsen, U.R., 2020. Nature as a treasure trove of potential anti-SARS-CoV drug leads: a structural/mechanistic rationale. RSC Advances. 10, 19790–19802. https://doi.org/10.1039/D0RA04199H

Shin, D., Mukherjee, R., Grewe, D., Bojkova, D., Baek, K., Bhattacharya, A., Schulz, L., Widera, M., Mehdipour, A.R., Tascher, G.J.N., 2020. Papain-like protease regulates SARS-CoV-2 viral spread and innate immunity. Nature Medicine. 587, 657–662. https://doi.org/10.1038/s41586-020-2601-5

Singh, P., Pathania, S., Rawal, R., 2020. Exploring RdRp-remdesivir interactions to screen RdRp inhibitors for the management of novel coronavirus 2019-nCoV. SAR and QSAR in Environmental Research. 31, 857–867. https://doi.org/10.1080/1062936x.2020.1825014

Son, J.K., Son, M.J., Lee, E., Moon, T.C., Son, K.H., Kim, C.H., Kim, H.P., Kang, S.S., Chang, H.W., 2005. Ginkgetin, a Biflavone from Ginko biloba leaves, inhibits cyclooxygenases-2 and 5-lipoxygenase in mouse bone marrow-derived mast cells. Biological and Pharmaceutical Bulletin. 28, 2181–2184. https://doi.org/10.1248/bpb.28.2181

Sun, C.M., Syu, W.J., Huang, Y.T., Chen, C.C., Ou, J.C., 1997. Selective cytotoxicity of ginkgetin from Selaginella moellendorffii. Journal of Natural Products. 60, 382–384. https://doi.org/10.1021/np960608e

Tamura, S., Yang, G.M., Yasueda, N., Matsuura, Y., Komoda, Y., Murakami, N., 2010. Tellimagrandin I, HCV invasion inhibitor from Rosae rugosae Flos. Bioorganic Medicinal Chemistry Letters. 20, 1598–1600. https://doi.org/10.1016/j.bmcl.2010.01.084

Tito, A., Colantuono, A., Pirone, L., Pedone, E.M., Intartaglia, D., Giamundo, G., Conte, I., Vitaglione, P., Apone, F., 2020. Pomegranate Peel Extract as an Inhibitor of SARS-CoV-2 Spike Binding to Human ACE2 Receptor (in vitro): A Promising Source of Novel Antiviral Drugs. Frontiers in Chemistry. 9, 638187. https://doi.org/10.3389/fchem.2021.638187

Trott, O., Olson, A.J., 2010. AutoDock Vina: improving the speed and accuracy of docking with a new scoring function, efficient optimization, and multithreading. Journal of computational chemistry. 31, 455–461. https://doi.org/10.1002/jcc.21334

Veber, D.F., Johnson, S.R., Cheng, H.Y., Smith, B.R., Ward, K.W., Kopple, K.D., 2002. Molecular properties that influence the oral bioavailability of drug candidates. Journal of Medicinal Chemistry. 45, 2615–2623. https://doi.org/10.1021/jm020017n

Venkataraman, S., Prasad, B.V., Selvarajan, R., 2018. RNA dependent RNA polymerases: insights from structure, function and evolution. Viruses. 10, 76. https://doi.org/10.3390/v10020076

V'kovski, P., Kratzel, A., Steiner, S., Stalder, H., Thiel, V., 2020. Coronavirus biology and replication: implications for SARS-CoV-2. Nature Reviews Microbiology. 19, 155–170. https://doi.org/10.1038/s41579-020-00468-6

Wang, M., Li, Y., Hu, X., 2018. Chebulinic acid derived from triphala is a promising antitumour agent in human colorectal carcinoma cell lines. BMC Complementary Alternative Medicine. 18, 342. https://doi.org/10.1186/s12906-018-2412-5

Williams, C.A., Harborne, J.B., Tomas-Barberan, F.A., 1987. Biflavonoids in the primitive monocots Isophysis tasmanica and Xerophyta plicata. Phytochemistry. 26(9), 2553–2555. https://doi.org/10.1016/S0031-9422(00)83875-3

Wilsky, S., Sobotta, K., Wiesener, N., Pilas, J., Althof, N., Munder, T., Wutzler, P., Henke, A., 2012. Inhibition of fatty acid synthase by amentoflavone reduces coxsackievirus B3 replication. Archives of Virology. 157, 259–269. https://doi.org/10.1007/s00705-011-1164-z

Woldemichael, G.M., Singh, M.P., Maiese, W.M., Timmermann, B.N., 2003. Constituents of antibacterial extract of Caesalpinia paraguariensis Burk. Zeitschrift für Naturforschung C. 58, 70–75. https://doi.org/10.1515/znc-2003-1-213

Xia, S., Liu, M., Wang, C., Xu, W., Lan, Q., Feng, S., Qi, F., Bao, L., Du, L., Liu, S., 2020. Inhibition of SARS-CoV-2 (previously 2019-nCoV) infection by a highly potent pan-coronavirus fusion inhibitor targeting its spike protein that harbors a high capacity to mediate membrane fusion. Cell Research. 30, 343–355. https://doi.org/10.1038/s41422-020-0305-x

Yang, S.Y., 2010. Pharmacophore modeling and applications in drug discovery: challenges and recent advances. Drug Discovery Today. 15, 444–450. https://doi.org/10.1016/j.drudis.2010.03.013

Yavuz, S., Ünal, S., 2020. Antiviral treatment of COVID-19. Turkish Journal of Medical Sciences. 50, 611–619. https://doi.org/10.3906/sag-2004-145

Yi, L., Li, Z., Yuan, K., Qu, X., Chen, J., Wang, G., Zhang, H., Luo, H., Zhu, L., Jiang, P., 2004. Small molecules blocking the entry of severe acute respiratory syndrome coronavirus into host cells. Journal of virology. 78, 11334–11339. https://doi.org/10.1128/jvi.78.20.11334-11339.2004

Zheng, S., Laraia, L., O'connor, C.J., Sorrell, D., Tan, Y.S., Xu, Z., Venkitaraman, A.R., Wu, W., Spring, D.R., 2012. Synthesis and biological profiling of tellimagrandin I and analogues reveals that the medium ring can significantly modulate biological activity. Organic & Biomolecular Chemistry. 10, 2590–2593. https://doi.org/10.1039/C2OB25065A